Robust Performance Analysis: a Review of Techniques for Dealing with Infinite Dimensional LMIs

Andreas Knoblach, Mehran Assanimoghaddam, Harald Pfifer and Florian Saupe

***Abstract*— This paper compares three techniques for dealing with infinite dimensional linear matrix inequalities (LMIs) for robust performance analysis: the gridding based approximation, the polytopic relaxation and the linear fractional representation based relaxation. The latter draws on the Full Block S-Procedure with different types of multipliers. All three techniques are applied in two benchmark studies at the example of an aeroelastic system. The studies are backed up by results from the Robust Control Toolbox for Matlab.**

I. Introduction

Robust performance analysis is a powerful tool to characterize uncertain and linear parameter-varying (LPV) systems based on input-output gains. The most common norm used in this framework is the induced $\mathcal{L}_2$ norm, which is also known as worst case energy-to-energy gain. Another important performance measure is the induced $\mathcal{L}_2$-$\mathcal{L}_\infty$ norm, which specifies the worst case energy-to-peak gain. Upper bounds for these norms can be computed by solving convex optimization problems whose constraints are formulated via linear matrix inequalities (LMIs), see e. g. [1], [2] and [3]. However, it is not straight forward to derive a numerically solvable formulation of the analysis problem. On the one hand, the decision variables can have an arbitrary functional dependence on the parameters of the considered system. On the other hand, the constraints depend on the system parameters, so that they are infinite dimensional. Both problems cause the optimization problem to be numerical intractable. Several remedies are proposed in the literature. The standard approach to avoid the functional dependence of the decision variables is to assign basis functions, restricting the function space. The coefficients of the basis functions are the new decision variables, see e. g. [4]. In order to yield a finite number of constraints, three approaches are proposed in the literature: The first approach is proposed in [4] and is based on an approximation of the entire parameter space using a finite number of grid points. The second one – commonly referred to as polytopic LPV approach – is restricted to LPV systems with affine parameter dependence, see [5]. Finally, the so called Full Block S-Procedure can be used if the LPV model is given in its linear fractional representation (LFR), see [2] and [6].

This paper aims on a neutral comparison of these methods and their several options. The focus of this paper lies on a benchmark study at the example of the performance analysis of a flexible restrained airfoil in a heaving and bending motion.

The authors are with the Institute of System Dynamics and Control, German Aero Space Center (DLR), 82234 Wessling, Germany andreas.knoblach@dlr.de.

The paper is structured as follows: Important preliminaries are repeated in Section II. LPV and LFR models are defined and LMI constraints representing two system norms are presented. Section III treats how tractable constraints can be derived from the LMIs. First, the assignment of basis functions is discussed. The approximation based on the gridding approach and the relaxation based on the polytopic approach are presented. The LFR based relaxation using the Full Bock S-Procedure is treated next. The two benchmark studies are presented in Section IV. The studies are backed up by results from the Robust Control Toolbox for Matlab, see [7].

II. Preliminaries

A. LPV and LFR Models

In order to introduce the class of LPV systems, differentiable parameter vector trajectories with bounded rates are defined first. The time dependent parameter vector is defined as a function $\boldsymbol{\rho}\colon \mathbb{R} \to \mathcal{P}$, where $\mathcal{P}$ is a compact subset of $\mathbb{R}^{n_\rho}$ and n_ρ is the number of scheduling signals. The vertices of the convex hull of $\mathcal{P}$ are denoted $\overline{\mathcal{P}}$. The variation rate of the parameters are bounded by $\dot{\boldsymbol{\rho}}\colon \mathbb{R} \to \dot{\mathcal{P}}$ with

$$\dot{\mathcal{P}} = \{\boldsymbol{q} \mid |q_i| \leq \nu_i \ \forall i \in \{1, \ldots, n_\rho\}\} \tag{1}$$

where ν_i is a non negative number. Consequently, the image space of $\dot{\boldsymbol{\rho}}(t)$ is a hyper-rectangle $\dot{\mathcal{P}} \subset \mathbb{R}^{n_\rho}$.

With the continuous matrix functions $\boldsymbol{A}\colon \mathcal{P} \to \mathbb{R}^{n_x \times n_x}$, $\boldsymbol{B}\colon \mathcal{P} \to \mathbb{R}^{n_x \times n_d}$, $\boldsymbol{C}\colon \mathcal{P} \to \mathbb{R}^{n_e \times n_x}$, $\boldsymbol{D}\colon \mathcal{P} \to \mathbb{R}^{n_e \times n_d}$, a state vector $\boldsymbol{x} \in \mathbb{R}^{n_x}$, an input vector $\boldsymbol{d} \in \mathbb{R}^{n_d}$ and an output vector $\boldsymbol{e} \in \mathbb{R}^{n_e}$, the linear parameter-varying (LPV) system $\boldsymbol{P}(\boldsymbol{\rho}(t))$ is according to [4] defined by

$$\boldsymbol{P}(\boldsymbol{\rho}(t))\colon \begin{cases} \dot{\boldsymbol{x}} = \boldsymbol{A}(\boldsymbol{\rho}(t))\boldsymbol{x} + \boldsymbol{B}(\boldsymbol{\rho}(t))\boldsymbol{d} \\ \boldsymbol{e} = \boldsymbol{C}(\boldsymbol{\rho}(t))\boldsymbol{x} + \boldsymbol{D}(\boldsymbol{\rho}(t))\boldsymbol{d}\,. \end{cases} \tag{2}$$

For convenience, the explicit dependence of $\boldsymbol{\rho}$ on t is dropped below.

Next, the linear fractional representation (LFR) is introduced. Using the partitioned matrix

$$\boldsymbol{M} = \left[\begin{array}{c|c} \boldsymbol{M}_{11} & \boldsymbol{M}_{12} \\ \hline \boldsymbol{M}_{21} & \boldsymbol{M}_{22} \end{array}\right] \in \mathbb{C}^{(n_1+n_2)\times(m_1+m_2)} \tag{3}$$

and the matrix $\boldsymbol{\Delta} \in \mathbb{C}^{m_1 \times n_1}$, the upper linear fractional transformation (LFT) is defined as

$$\mathcal{F}(\boldsymbol{M}, \boldsymbol{\Delta}) = \boldsymbol{M}_{22} + \boldsymbol{M}_{21}\boldsymbol{\Delta}(\mathbf{I} - \boldsymbol{M}_{11}\boldsymbol{\Delta})^{-1}\boldsymbol{M}_{12}, \tag{4}$$

Preprint submitted to 2013 IEEE Multi-conference on Systems and Control.
Received February 28, 2013.

see [8]. For every rational function $\boldsymbol{F}\colon \mathcal{P} \to \mathbb{R}^{n_2 \times m_2}$ depending on a parameter vector $\boldsymbol{\rho} = \begin{bmatrix}\rho_1 & \dots & \rho_{n_\rho}\end{bmatrix}$ an LFR can be found, i. e. a matrix $\boldsymbol{M}$ and a linear function

$$\boldsymbol{\Delta}(\boldsymbol{\rho}) = \operatorname{diag}(\rho_1 \mathbf{I}_{s_1}, \dots, \rho_{n_\rho} \mathbf{I}_{s_{n_\rho}}) \tag{5}$$

s. t.

$$\boldsymbol{F}(\boldsymbol{\rho}) = \mathcal{F}\left(\boldsymbol{M}, \boldsymbol{\Delta}(\boldsymbol{\rho})\right). \tag{6}$$

The positive integers s_i determine how often the parameter ρ_i is repeated in the $\boldsymbol{\Delta}$-block. Without loss of generality, the parameters ρ_i are typically scaled s. t. $\rho_i \in [-1, 1] \ \forall i \in \{1, \dots, n_\rho\}$, see [8] for details.

B. Robust Performance Analysis

The idea of robust performance analysis is to characterize the properties of the LPV system by worst case input-output

$$\|\boldsymbol{P}(\boldsymbol{\rho})\|_{m,n} = \sup_{\|\boldsymbol{w}(t)\|_m \neq 0} \frac{\|\boldsymbol{e}(t)\|_n}{\|\boldsymbol{w}(t)\|_m} \tag{7}$$

gains for all admissible parameter trajectories. Since the parameter vector trajectories of the system are not known a priori, the major idea is to check the parameter space $\mathcal{P} \times \dot{\mathcal{P}}$ instead of the trajectories. For that reason, the auxiliary variables $\boldsymbol{p} \in \mathcal{P}$ and $\boldsymbol{q} \in \dot{\mathcal{P}}$ are introduced.

For convenience, two abbreviations will be used. First, the differential operator $\partial\boldsymbol{X}\colon \mathcal{P} \times \dot{\mathcal{P}} \to \mathbb{S}^{n_x}$ is defined as

$$\partial\boldsymbol{X}(\boldsymbol{p}, \boldsymbol{q}) = \sum_{i=1}^{n_\rho} \frac{\partial \boldsymbol{X}(\boldsymbol{p})}{\partial p_i} q_i, \tag{8}$$

where $\boldsymbol{X}\colon \mathcal{P} \to \mathbb{S}^{n_x}$ is a continuously differentiable matrix function.[1] The second one, $[*]$ will be used to denote large symmetric matrix expressions, e. g.

$$[*]\,\boldsymbol{T}\boldsymbol{F} = \boldsymbol{F}^{\mathrm{T}}\boldsymbol{T}\boldsymbol{F}, \quad \text{where } \boldsymbol{T} \in \mathbb{S}. \tag{9}$$

With these definitions, LMI constraints for the worse case energy-to-energy gain and for the worse case energy-to-peak gain are given below. Constraints for further performance measures can be found in e. g. [1] and [2].

1) Energy-to-Energy Gain: The LPV system $\boldsymbol{P}(\boldsymbol{\rho})$ is exponential stable and its induced $\mathcal{L}_2$ norm[2] $\|\boldsymbol{P}(\boldsymbol{\rho})\|_{2,2}$ from $\boldsymbol{d}$ to $\boldsymbol{e}$ is smaller than a performance index γ if there exists a Lyapunov matrix $\boldsymbol{X}\colon \mathcal{P} \to \mathbb{S}^{n_x}$ s. t. $\forall(\boldsymbol{p}, \boldsymbol{q}) \in \mathcal{P} \times \dot{\mathcal{P}}$

$$\boldsymbol{X}(\boldsymbol{p}) > 0, \tag{10a}$$

$$[*]\left[\begin{array}{cc|cc} \partial\boldsymbol{X}(\boldsymbol{p},\boldsymbol{q}) & \boldsymbol{X}(\boldsymbol{q}) & \mathbf{0} & \mathbf{0} \\ \boldsymbol{X}(\boldsymbol{q}) & \mathbf{0} & \mathbf{0} & \mathbf{0} \\ \hline \mathbf{0} & \mathbf{0} & -\mathbf{I} & \mathbf{0} \\ \mathbf{0} & \mathbf{0} & \mathbf{0} & \frac{1}{\gamma^2}\mathbf{I} \end{array}\right]\left[\begin{array}{cc} \mathbf{I} & \mathbf{0} \\ \boldsymbol{A}(\boldsymbol{p}) & \boldsymbol{B}(\boldsymbol{p}) \\ \hline \mathbf{0} & \mathbf{I} \\ \boldsymbol{C}(\boldsymbol{p}) & \boldsymbol{D}(\boldsymbol{p}) \end{array}\right] < 0, \tag{10b}$$

see [2]. An upper bound for $\|\boldsymbol{P}(\boldsymbol{\rho})\|_{2,2}$ can be determined by solving the optimization problem

$$\min_{\gamma, \boldsymbol{X}(\boldsymbol{p})} \gamma \quad \text{s. t. (10) is fulfilled.} \tag{11}$$

Since γ does not appear affinely in the constraints, $-\frac{1}{\gamma^2}$ is instead used as decision variable and as objective in practice.

[1] $\mathbb{S}^n \subset \mathbb{R}^{n \times n}$ denotes the set of symmetric matrices.

[2] In the LTI case, this norm corresponds to the $\mathcal{H}_\infty$ norm.

2) Energy-to-Peak Gain: The LPV system $\boldsymbol{P}(\boldsymbol{\rho})$ with $\boldsymbol{D}(\boldsymbol{\rho}) = \mathbf{0}$ is exponential stable and its induced $\mathcal{L}_2$-$\mathcal{L}_\infty$ norm[3] $\|\boldsymbol{P}(\boldsymbol{\rho})\|_{2,\infty}$ from $\boldsymbol{d}$ to $\boldsymbol{e}$ s smaller than a performance index γ if there exists a Lyapunov matrix $\boldsymbol{X}\colon \mathcal{P} \to \mathbb{S}^{n_x}$ s. t. $\forall(\boldsymbol{p}, \boldsymbol{q}) \in \mathcal{P} \times \dot{\mathcal{P}}$

$$\boldsymbol{X}(\boldsymbol{p}) > 0, \tag{12a}$$

$$[*]\left[\begin{array}{cc|cc} \partial\boldsymbol{X}(\boldsymbol{p},\boldsymbol{q}) & \boldsymbol{X}(\boldsymbol{q}) & \mathbf{0} & \mathbf{0} \\ \boldsymbol{X}(\boldsymbol{q}) & \mathbf{0} & \mathbf{0} & \mathbf{0} \\ \hline \mathbf{0} & \mathbf{0} & -\gamma\mathbf{I} & \mathbf{0} \\ \mathbf{0} & \mathbf{0} & \mathbf{0} & -\gamma\mathbf{I} \end{array}\right]\left[\begin{array}{cc} \mathbf{I} & \mathbf{0} \\ \boldsymbol{A}(\boldsymbol{p}) & \boldsymbol{B}(\boldsymbol{p}) \\ \hline \mathbf{0} & \mathbf{I} \\ \boldsymbol{C}(\boldsymbol{p}) & \boldsymbol{D}(\boldsymbol{p}) \end{array}\right] < 0, \tag{12b}$$

$$[*]\left[\begin{array}{c|ccc} \boldsymbol{X}(\boldsymbol{p}) & \mathbf{0} & \mathbf{0} & \mathbf{0} \\ \hline \mathbf{0} & \gamma\mathbf{I} & \mathbf{0} & \mathbf{0} \\ \mathbf{0} & \mathbf{0} & \mathbf{0} & \mathbf{I} \\ \mathbf{0} & \mathbf{0} & \mathbf{I} & \mathbf{0} \end{array}\right]\left[\begin{array}{cc} \mathbf{I} & \mathbf{0} \\ \hline \mathbf{0} & \mathbf{I} \\ \boldsymbol{C}(\boldsymbol{p}) & \mathbf{0} \\ \mathbf{0} & \mathbf{I} \end{array}\right] > 0. \tag{12c}$$

The proof for the linear time invariant (LTI) case in [2] can be easily extended to LPV systems. This leads to the following optimization problem for computing an upper bound for $\|\boldsymbol{P}(\boldsymbol{\rho})\|_{2,\infty}$:

$$\min_{\gamma, \boldsymbol{X}(\boldsymbol{p})} \gamma \quad \text{s. t. (12) is fulfilled.} \tag{13}$$

III. Deriving a Tractable Solution

It is shown first how the arbitrary functional dependence of the decision variable $\boldsymbol{X}(\boldsymbol{p})$ can be circumvented by assigning basis functions. Next, three different techniques for dealing with the infinite dimensional constraints are explained and compared.

A. Basis Functions for the Lyapunov Matrix

In order to avoid the functional dependency of the decision variable, Wu [4] proposed to assign n_f basis function

$$\boldsymbol{X}(\boldsymbol{p}) = \sum_{i=1}^{n_\mathrm{f}} \mathrm{f}_i(\boldsymbol{p}) \boldsymbol{X}_i, \quad \text{where } \boldsymbol{X}_i \in \mathbb{S}^{n_x}. \tag{14}$$

The new decision variables are the coefficients of the basis functions $\boldsymbol{X}_i$.

More basis functions obviously reduce the conservatism. However, since every basis function increases the number of the decision variables, this slows the optimization process down or may cause severe numerical problems. Consequently, the selection of the basis functions is an important step, which can have a crucial effect on the results. Unfortunately, there are hardly any guidelines in literature how to do this, but simple polynomials lead to good results in practice.

B. Approximation Based on Gridding the Parameter Space

The simplest and maybe most popular way to circumvent infinite dimensional LMIs is introduced in [4] and is based on a gridding of the parameter space. This means that the constraints are only enforced on a finite subset $\mathcal{P}_\mathrm{grid} \subset \mathcal{P}$. Since $\dot{\mathcal{P}}$ is a polytope and the parameter $\boldsymbol{q} \in \dot{\mathcal{P}}$ enters the constraints only affinely, it is sufficient to check the constraints only at the vertices $\operatorname{vert}(\dot{\mathcal{P}})$, see [1]. This gridding approach

[3] In the LTI case, this norm corresponds to the generalized $\mathcal{H}_2$ norm.

Preprint submitted to 2013 IEEE Multi-conference on Systems and Control.
Received February 28, 2013.

is thus based on an approximation of the original parameter space $\mathcal{P} \times \dot{\mathcal{P}}$ by $\mathcal{P}_{\text{grid}} \times \text{vert}(\dot{\mathcal{P}})$.

Because this is a mere approximation of the original problem, sufficiency is lost. It is thus self-explanatory that the density of the grid must be carefully chosen. In order to check the validity of the results, it is possible to optimize the performance index again with the obtained Lyapunov matrix on a second, much finer grid. A slight increase of the new performance index indicates – but does not prove – the validity of the results. However, the fact that sufficiency is lost should not be overrated. Even in the μ-framework, the analysis if often performed on a finite grid of frequency points.

C. Relaxation Based on Polytopes

The following relaxation is restricted to LPV systems which depend only affinely on the parameters, e. g.

$$\boldsymbol{A}(\boldsymbol{\rho}) = \boldsymbol{A}_0 + \sum_{i=1}^{n_\rho} \rho_i \boldsymbol{A}_i \tag{15}$$

and analogously for the other system matrices. In contrast to the common literature (e. g. [5]), not only a constant Lyapunov matrix but one which depends also affinely on the parameters is considered here. In this case, the constraints (10) and (12) are fulfilled if the constraints hold on the vertices of the convex hull of the parameter space $\overline{\mathcal{P}} \times \text{vert}(\dot{\mathcal{P}})$ and if

$$\left[\begin{array}{c|c} \boldsymbol{A}_i^{\mathrm{T}}\boldsymbol{X}_i + \boldsymbol{X}_i\boldsymbol{A}_i & \boldsymbol{X}_i\boldsymbol{B}_i \\ \hline \boldsymbol{B}_i^{\mathrm{T}}\boldsymbol{X}_i & \boldsymbol{0} \end{array}\right] \geq 0 \quad \forall i = 1, \dots n_\rho. \tag{16}$$

The last condition (16) enforces that the constraints are partially convex[4] in the parameter vector $\boldsymbol{\rho}$. It is thus sufficient to check the constraints at the vertices of the parameter space $\overline{\mathcal{P}}$. A more detailed derivation can be found in [3].

D. Relaxation Based on the Full Block S-Procedure

The last relaxation method is based on an LFR of the LPV model and of the basis functions for the Lyapunov matrix. The Full Block S-Procedure is a result from linear algebra which allows relaxing matrix inequalities of the from

$$\boldsymbol{F}(\boldsymbol{p})^{\mathrm{T}}\boldsymbol{T}\boldsymbol{F}(\boldsymbol{p}) < 0, \tag{17}$$

where $\boldsymbol{T} \in \mathbb{S}^{n_2}$ and $\boldsymbol{F}(\boldsymbol{p}) = \mathcal{F}(\boldsymbol{M}, \boldsymbol{\Delta}(\boldsymbol{p}))$, see [6]. The condition (17) holds if and only if there exists a general multiplier $\boldsymbol{\Pi} \in \mathbb{S}^{2n_1}$ s. t.

$$\left[\begin{array}{cc} \boldsymbol{M}_{11} & \boldsymbol{M}_{12} \\ \mathbf{I} & \mathbf{0} \\ \hline \boldsymbol{M}_{21} & \boldsymbol{M}_{22} \end{array}\right]^{\mathrm{T}} \text{diag}(\boldsymbol{\Pi}, \boldsymbol{T}) \left[\begin{array}{cc} \boldsymbol{M}_{11} & \boldsymbol{M}_{12} \\ \mathbf{I} & \mathbf{0} \\ \hline \boldsymbol{M}_{21} & \boldsymbol{M}_{22} \end{array}\right] < 0 \tag{18}$$

and $\forall \boldsymbol{p} \in \mathcal{P}$

$$\begin{bmatrix} \mathbf{I} \\ \boldsymbol{\Delta}(\boldsymbol{p}) \end{bmatrix}^{\mathrm{T}} \boldsymbol{\Pi} \begin{bmatrix} \mathbf{I} \\ \boldsymbol{\Delta}(\boldsymbol{p}) \end{bmatrix} \geq 0. \tag{19}$$

The relaxation is thus achieved by introducing additional decision variables in the form of the multiplier $\boldsymbol{\Pi}$.

[4] A constraint is partial convex if the function describing the constraint is convex in each of its parameter.

1) Structure of Multipliers: In order to relax the still infinite dimensional second constraint (19), the structure of the multiplier is restricted. The two types of multipliers introduced below are based on the structure

$$\boldsymbol{\Pi} = \begin{bmatrix} \boldsymbol{Q} & \boldsymbol{S} \\ \boldsymbol{S}^{\mathrm{T}} & \boldsymbol{R} \end{bmatrix}, \quad \text{where } \boldsymbol{Q}, \boldsymbol{R} \in \mathbb{S}^{n_1}. \tag{20}$$

First, the so called diagonal multipliers are introduced. Assuming

$$\begin{aligned} &\boldsymbol{R} = \text{diag}(\boldsymbol{R}_1, \dots, \boldsymbol{R}_{n_\rho}) \leq 0, \quad \text{where } \boldsymbol{R}_i \in \mathbb{S}^{s_i}, \\ &\boldsymbol{Q} = -\boldsymbol{R}, \\ &\boldsymbol{S} = \text{diag}(\boldsymbol{S}_1, \dots, \boldsymbol{S}_{n_\rho}), \quad \text{where } \boldsymbol{S}_i = -\boldsymbol{S}_i^{\mathrm{T}} \in \mathbb{R}^{s_i \times s_i} \end{aligned} \tag{21}$$

and using the structure of the $\boldsymbol{\Delta}$-block (5), it is easy to prove that the second constraint (19) is always fulfilled. A special case is $\boldsymbol{S} = \mathbf{0}$, where the number of decision variables is reduced of the price of more conservatism.

An other type of multipliers are the full block multipliers. Using the structure (20) with $\boldsymbol{R} \leq 0$, the second constraint (19) becomes concave. Since the set of all possible $\boldsymbol{\Delta}$-blocks is a convex hull (cf. (5)), it is sufficient to check (19) at the vertices of this hull, denoted by $\overline{\mathcal{P}}$.

Note that diagonal multipliers are a subset of the full block multipliers. Hence, the latter are supposed to be less conservative. However, they introduce more additional decision variables and increase the number of LMIs. Further details on multipliers and other types of multipliers can be found in [9].

2) LFR of Lyapunov Basis Functions: In order to use the Full Block S-Procedure, it is necessary to write the Lyapunov basis functions as

$$\boldsymbol{X}(\boldsymbol{p}) = \boldsymbol{F}_X(\boldsymbol{p})^{\mathrm{T}}\boldsymbol{T}_X\boldsymbol{F}_X(\boldsymbol{p}), \tag{22}$$

where the basis functions are defined by $\boldsymbol{F}_X(\boldsymbol{p})$ and their coefficients are collected in $\boldsymbol{T}_X \in \mathbb{S}$. The differential operator becomes

$$\partial\boldsymbol{X}(\boldsymbol{p}, \boldsymbol{q}) = [*] \begin{bmatrix} \mathbf{0} & \boldsymbol{T}_X \\ \boldsymbol{T}_X & \mathbf{0} \end{bmatrix} \begin{bmatrix} \partial\boldsymbol{F}_X(\boldsymbol{p}, \boldsymbol{q}) \\ \boldsymbol{F}_X(\boldsymbol{p}) \end{bmatrix}. \tag{23}$$

E. Comparison of the Techniques

The severest drawback of the gridding approach is that there are no guarantees. Another problem is that the number of grid points (and thus the number of LMIs) grows exponentially with the number of scheduling parameters. The drawback of the LFR based approach is the number of additional decision variables. Especially for parameter dependent Lyapunov matrices of systems with many states, the $\boldsymbol{\Delta}$-block grows rapidly. Since this introduces many additional decision variables, such problems become quickly intractable. The gridding approach is thus attractive for systems whose state space matrices have a complex – probably non-rational – dependency on a few parameters. For models with a simple dependence on many parameters and a low number of states the LFR based approach is preferable.

The polytopic approach is restricted to affine parameter dependent LPV systems. While every LPV system can be over-bounded by such an affine parameter dependent LPV model, this approach is usually extremely conservative [4].

Preprint submitted to 2013 IEEE Multi-conference on Systems and Control.
Received February 28, 2013.

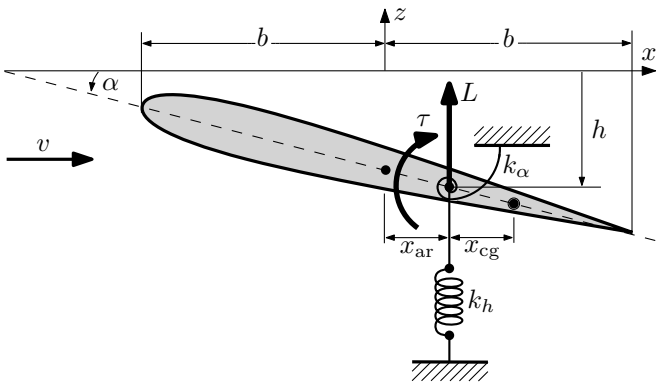

Fig. 1. Aeroelastic system; figure adapted from [14].

IV. Performance Analysis of a Flexible Restrained Airfoil

This section provides a benchmark study of the different approaches. First, some information how the analysis is implemented is presented. Next, the considered aeroelastic model is introduced. Afterwards, two scenarios are considered.

A. Implementation of the Analysis

The analysis is performed using Matlab. In order to obtain a minimum order of the LFR models, the DLR/ONERA LFR toolbox is used, see [10]. The LMIs are coded using Yalmip, see [11]. Except for three cases in the second scenario (cf. Table III) the LMI solver SDPT3 [12] yield the best results, while SeDuMi [13] found often only an infeasible solution. However, in these three cases, SeDuMi obtained a feasible solution.

B. Model of the Aeroelastic System

The considered aeroelastic system is taken from [14]. It is illustrated in Fig. 1. The equations of motion are

$$\begin{bmatrix} m & m \cdot x_{\text{cg}} \\ m \cdot x_{\text{cg}} & I \end{bmatrix} \begin{bmatrix} \ddot{h} \\ \ddot{\alpha} \end{bmatrix} + \begin{bmatrix} k_h & 0 \\ 0 & k_\alpha \end{bmatrix} \begin{bmatrix} h \\ \alpha \end{bmatrix} = \begin{bmatrix} -L \\ \tau \end{bmatrix}, \quad (24)$$

where h denotes the vertical deflection and α the pitch angle. The lift L and the pitching moment τ are given by

$$\begin{bmatrix} -L \\ \tau \end{bmatrix} = \tfrac{1}{2}\rho v^2 \left[\boldsymbol{Q}_{\text{eig}} \mid \boldsymbol{Q}_{\text{gust}} \right] \left[\begin{array}{c} h \\ \alpha \\ \hline w \end{array} \right]. \quad (25)$$

TABLE I
Model parameters: explanation and default values

Sym.	Explanation	Value
k_h	translational stiffness	0.04
k_α	rotational stiffness	0.25
m	mass	1.00
I	inertia	0.25
x_{cg}	location of the center of gravity	0.20
v	free stream velocity	0.70
ρ	air density	0.80
b	half chord length	1.00
x_{ar}	location of the aerodynamic reference axis	−0.20

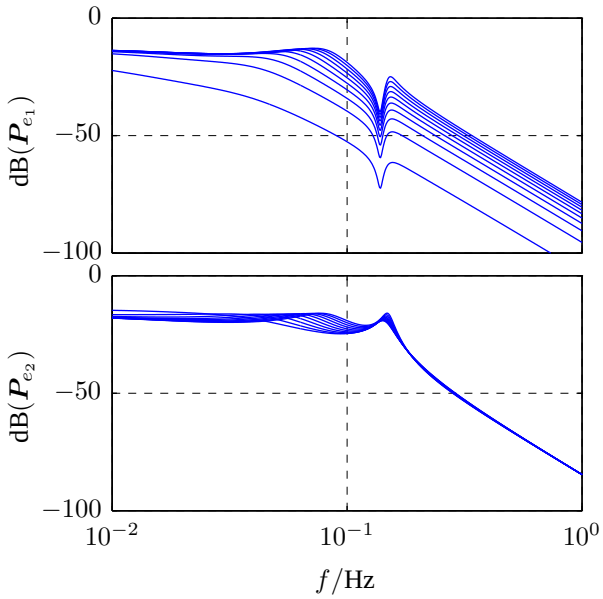

Fig. 2. Bode diagram of scenario 1 (10 values of k_h)

The Theodorsen function $\boldsymbol{Q}_{\text{eig}}$ models the relation between the aerodynamic forces and the eigen movement. The Küssner function $\boldsymbol{Q}_{\text{gust}}$ maps the vertical gust velocity w on L and τ. For both non-rational functions, R. T. Jones' approximations are used in order to yield a state space realization. Both functions depend on the free stream velocity v, the half chord length b and the location of the aerodynamic reference axis x_{ar}. Default values and explanations for all model parameters are given in Table I.

In the considered scenarios, the model input is the gust velocity $d = w$ and the outputs are the spring forces

$$\boldsymbol{e} = \begin{bmatrix} k_h \cdot h \\ k_\alpha \cdot \alpha \end{bmatrix}. \quad (26)$$

Since the parameter dependence of the resulting state space model is highly involved, it is not explicitly given. However, it has eight states and the feed through matrix is zero.

C. Scenario 1: Uncertain Translational Stiffness

In the first scenario, the translational stiffness is assumed to be uncertain in the range of $k_h \in [0.01, 0.30]$. In order to allow a meaningful comparison with LTI results, the parameter rate is set to zero. The LPV model depends only affinely on the single parameter and the $\boldsymbol{\Delta}$-block is scalar. The bode diagram of the resulting system is depicted in Fig. 2 for ten values of k_h.

The analysis results are presented in Table II. In case of a constant Lyapunov matrix, the constraints for both norms are infeasible, independent of the relaxation method. The gridding-based and the LFR-based analysis yield in all cases the same results. For an affine parameter dependent Lyapunov matrix, the worst case energy-to-energy gain is 5 % greater and the worst case energy-to-peak gain is 17 % greater than

Preprint submitted to 2013 IEEE Multi-conference on Systems and Control.
Received February 28, 2013.

the LTI norm of the worst grid point.[5] In case of a quadratic parameter dependent Lyapunov matrix, both norms are only slightly greater than the maximum LTI norm. Consequently, no higher order polynomial are considered as basis function. Although the considered model can be covered by a polytopic model without any overbounding, the result for the energy-to-energy gain using an affine parameter dependent Lyapunov matrix and the polytopic relaxation is extremely conservative. This can be caused only by the additional constraint (16) and seems to be a systematic problem of this approach. Finally, the results for the worst case energy-to-energy gain are compared to results from the function `wcgain` of the Robust Control Toolbox, see [7]. The result is the same as in case of the quadratic parameter dependent Lyapunov matrix.

TABLE II
RESULTS FOR SCENARIO 1

$\boldsymbol{X}(\rho)$	Relaxation	Norm $\|\boldsymbol{P}\|_{2,2}$	Norm $\|\boldsymbol{P}\|_{2,\infty}$
Const.	grid-based/polytopic/LFR-based	infeasible	
Affine	grid-based (10 points)	0.291	0.124
Affine	polytopic	0.597	0.129
Affine	LFR based (diag. multiplier)	0.291	0.124
Quad.	grid-based (10 points)	0.277	0.107
Quad.	LFR based (diag. multiplier)	0.277	0.107
Max. LTI norm of 100 grid points		0.276	0.107
Worst case gain of RCT		0.277	N/A

D. Scenario 2: Uncertain Mass und Velocity

In the second scenario, the mass is assumed to be uncertain in the interval $m \in [0.4, 1.5]$ and the free stream velocity in the range of $v \in [0.5, 0.8]$. The parameter rates are again set to zero. This leads to the $\boldsymbol{\Delta}$-block $\mathrm{diag}(m\mathbf{I}_3,\, v\mathbf{I}_7)$. The Bode diagram for the resulting model family is depicted in Fig. 3 for three different values per uncertain parameter. Because of the complex dependence of the model on the velocity v, an enormous overbounding is necessary to yield a polytopic LPV model. Since this causes an extreme conservatism, this approach is not considered in the following.

The analysis results are shown in Table III. Any analysis based on a Lyapunov matrix depending on only one parameter yield an infeasible problem. Using Lyapunov matrices which depend affinely on both parameters lead to results between 100 % and 115 % of the maximum LTI norm in case of the gridding approach and between 105 % and 150 % in case of an LFR based analysis. In case of quadratic parameter dependent Lyapunov matrices, the LPV analysis leads to almost the same results as the maximum LTI norms.

A first important result is that – in all cases – the grid based results with 10×10 points are identical to the results with 20×20 points. This indicates that the considered grid is dense enough. Since there are four times more grid points in the second case, the analysis lasts up to nine times longer.

[5]The LTI induced $\mathcal{L}_2$ norm is computed by the function `norm` of Matlab. The LTI induced $\mathcal{L}_2$-$\mathcal{L}_\infty$ norm is obtain by solving (13) for constant system matrices. Due to speed advantages for small LMI systems, this is done by LMI Lab, see [7]. Of course, the LTI results provide only a lower bound for the considered norms.

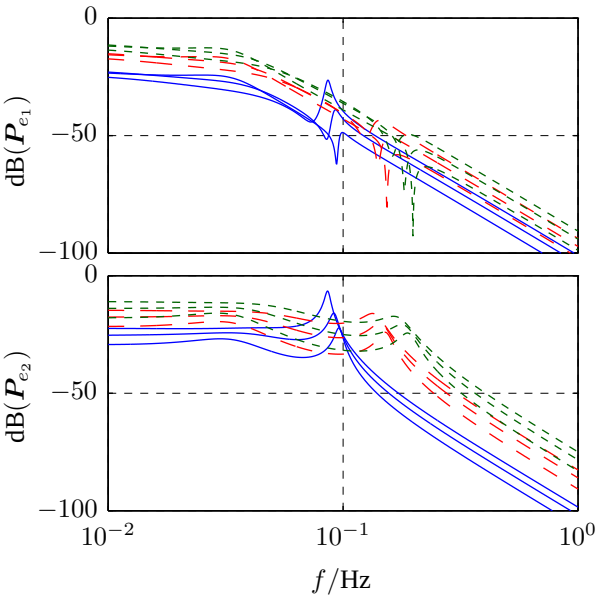

Fig. 3. Bode diagram of scenario 2 (3×3 values of v and k; the same line style indicates the same velocity v.)

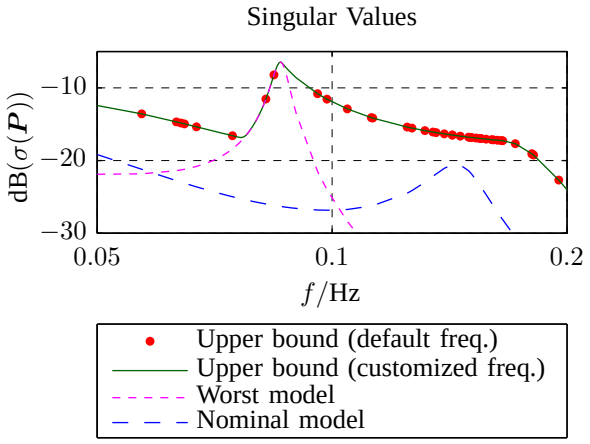

Fig. 4. Worst case gain analysis for scenario 2

With respect to the LFR based analysis, it can be said that diagonal multipliers outperform the full block multipliers. Although the diagonal multipliers are a subset of the full block multipliers, there is only one case in which the latter yield better results. In most of the other cases, they perform even worse, which is probably caused by numerical problems. Further, the computation time using the full block multipliers is up to 17 times longer than for the diagonal multipliers. Consequently, full block multipliers seem to be unattractive in practice – especially for more complex models.

Finally, it is mentioned that the default frequency grid of `wcgain` yields an upper bound which is smaller than the maximum LTI norm. In order to yield consistent results, it was necessary to use 2000 logarithmically space frequency points

Preprint submitted to 2013 IEEE Multi-conference on Systems and Control.
Received February 28, 2013.

TABLE III
RESULTS FOR SCENARIO 2

$\boldsymbol{X}(\rho)$	Relaxation	Norm $\|\boldsymbol{P}\|_{2,2}$	Norm $\|\boldsymbol{P}\|_{2,\infty}$	Comp. Time $\|\boldsymbol{P}\|_{2,2}$	Comp. Time $\|\boldsymbol{P}\|_{2,\infty}$
Const.	grid-based/LFR-based	infeasible		N/A	
Quad. in v	grid-based/LFR-based	infeasible		N/A	
Quad. in k	grid-based/LFR-based	infeasible		N/A	
Affine in v and k	grid-based (10×10 points)	0.477	0.133	8 s	12 s
Affine in v and k	grid-based (20×20 points)	0.477	0.133	37 s	64 s
Affine in v and k	LFR based (diagonal multiplier)	0.710	0.169	10 s	15 s
Affine in v and k	LFR based (full block multiplier)	0.499	0.172	174 s	246 s
Quad. in v and k	grid-based (10×10 points)	0.477	0.116*	10 s	18 s
Quad. in v and k	grid-based (20×20 points)	0.477	0.116*	90 s	115 s
Quad. in v and k	LFR based (diagonal multiplier)	0.477	0.118*	13 s	40 s
Quad. in v and k	LFR based (full block multiplier)	0.486	0.125	224 s	295 s
Max. LTI norm of 50×50 grid points		0.476	0.116	9 s	36 s
Worst case gain of RCT (default frequency grid)		0.388	N/A	26 s	N/A
Worst case gain of RCT (customized frequency grid)		0.477	N/A	262 s	N/A

*This result is obtained by SeDuMi.

between $0.01\,\text{Hz}$ and $1.00\,\text{Hz}$. The reason for the sensitivity toward the frequency grid is the distinct resonance of the system. See also Fig. 4.

V. SUMMARY AND OUTLOOK

Two comparative benchmark studies for the relaxation of infinite dimensional LMI constraints are presented. The first important result is that in the considered example the polytopic approach – independent of any overbounding during the modeling – is very conservative. Using the LFR based analysis, the diagonal multipliers clearly outperform the full block multipliers. The gridding based analysis leads to results which are consistent with the LFR based analysis. Since the LFR based relaxation obtains a guaranteed upper bound for the considered norm, it is convenient to use this approach. However, in case of models which depend very complex on only a few parameters, this approach may yield a too complex LMI system, see e. g. [15]. In such cases, the grid based approximation can be a reasonable option.

The most important advantage of the LPV performance analysis is that non-zero parameter rates can be considered. The influence of such non-zero rates has to be investigated in further studies. An other open questions is how the grid density can be chosen in order to obtain reliable results. In many cases, there appear numerical problems while solving the optimization problems. A scaling of the constraints and unknowns may help, but up to date no suitable strategies have been proposed.

REFERENCES

[1] Stephen Boyd, Laurent El Ghaoui, Eric Feron, and Venkataramanan Balakrishnan. *Linear Matrix Inequalities in System and Control Theory*. SIAM Studies in Applied Mathematics. Society for Industrial and Applied Mathematics, 1994.

[2] Marco Dettori. *LMI techniques for control with application to a Compact Disc player mechanism*. PhD thesis, Technische Universiteit Delft, 2001.

[3] Carsten Scherer and Siep Weiland. *Linear Matrix Inequalities in Control*. Delft Center for Systems and Control; Delft University of Technology, 2004.

[4] Fen Wu. *Control of Linear Parameter Varying Systems*. PhD thesis, University of California at Berkeley, 1995.

[5] Pierre Apkarian, Pascal Gahinet, and Greg Becker. Self-scheduled H_∞ control of linear parameter-varying systems: a design example. *Automatica*, 31(9):1251 – 1261, 1995.

[6] Fen Wu and Ke Dong. Gain-scheduling control of LFT systems using parameter-dependent lyapunov functions. *Automatica*, 42:39 – 50, 2006.

[7] Gary Balas, Richard Chiang, Andy Packard, and Michael Safonov. Robust control toolbox: User's guid, 2011.

[8] Simon Hecker. *Generation of low order LFT-Representations for Robust Control Applications*. PhD thesis, Fakultät für Elektrotechnik and Informationstechnik der Technischen Universität München, 2006.

[9] Harald Pfifer. *LPV/LFT Modeling and its Application in Aerospace*. PhD thesis, Technische Universität München, 2012.

[10] Simon Hecker, Andreas Varga, and Jean-Françoi Magni. Enhanced LFR-toolbox for MATLAB. *Aerospace Science and Technology, Elsevier*, 9:173 – 180, 2005.

[11] Johan Löfberg. Yalmip: A toolbox for modeling and optimization in MATLAB. In *Proceedings of the CACSD Conference*, 2004.

[12] Kim-Chuan Toh, Michael J. Todd, and Reha H. Tütüncü. Sdpt3 – a matlab software package for semidefinite programming. *Optimization Methods and Software*, 11:545 – 581, 1999.

[13] Jos F. Sturm. Using sedumi 1.02, a MATLAB toolbox for optimization over symmetric cones. *Optimization Methods and Software*, 11:625 – 653, 1999.

[14] Raymond L. Bisplinghoff, Holt Ashley, and Robert L. Halfman. *Aeroelasticity*. Dover Pubns, 1955.

[15] Andreas Knoblach. Robust performance analysis applied in loads computation of flexible aircrafts. Accepted and to be presented at the IFASD 2013.

Preprint submitted to 2013 IEEE Multi-conference on Systems and Control.
Received February 28, 2013.